Struct Multidisc Optim (2016) 53:15–27
DOI 10.1007/s00158-015-1308-y

RESEARCH PAPER

Multidisciplinary dynamic optimization of horizontal axis wind turbine design

Anand P. Deshmukh[1] · **James T. Allison**[1]

Received: 5 December 2014 / Revised: 11 April 2015 / Accepted: 21 July 2015 / Published online: 22 August 2015
© Springer-Verlag Berlin Heidelberg 2015

Abstract The design of physical (plant) and control aspects of a dynamic system have traditionally been treated as two separate problems, often solved in sequence. Optimizing plant and control design disciplines separately results in sub-optimal system designs that do not capitalize on the synergistic coupling between these disciplines. This coupling is inherent in most actively controlled dynamic systems, including wind turbines. In this case structural and control design both affect energy production and loads on the turbine. This article presents an integrated approach to achieve system-optimal wind turbine designs using co-design, a design methodology that accounts directly for the synergistic coupling between physical and control system design. A case study, based on multidisciplinary simulation, is presented here that demonstrates a promising increase (up to 8%) in annualized wind turbine energy production compared to the results of a conventional sequential design strategy. The case study also revealed specific synergistic mechanisms that enable performance improvements, which are accessible via co-design but not sequential design.

Keywords Wind Turbines · Structural Design · Optimal Control · Dynamic Optimization

Originally presented at 9th AIAA MDO Specialist Conference

✉ Anand P. Deshmukh
adeshmu2@illinois.edu

[1] Engineering Systems Design Laboratory, University of Illinois at Urbana–Champaign, 104 S Mathews Ave, Urbana, IL 61801, USA

Nomenclature

P_w	Rotor power, W
v	Instantaneous wind speed, m/s
v_i	Cut–in wind speed, m/s
v_o	Cut-out wind speed, m/s
$\mathbf{x_p}$	Plant design vector
T_r	Rotor torque, N·m
T_g	Generator torque, N·m
η	Gear ratio
J_r	Rotor inertia, kg·m^2
J_g	Generator side inertia, kg·m^2
B_r	Rotor torsional damping, N·m/rad/s
B_g	Generator side torsional damping, N·m/rad/s
Ω_r	Rotor speed, RPM
Ω_h	Speed on high-speed side (Generator), RPM
β	Blade pitch angle, deg
H_t	Tower height at the rotor hub, m
R_r	Turbine rotor radius, m
R_h	Turbine blade hub radius, m
D_r	Turbine rotor diameter, m
D_h	Turbine blade hub diameter, m
C_P	Rotor power coefficient
C_Q	Rotor torque coefficient
λ	Blade tip–speed ratio
ρ	Air density, kg/m^3
AEP	Annualized energy production, kW·h

1 Introduction

Wind energy is proving to be a promising source of renewable energy, complementing conventional energy systems to meet global energy demands. It is currently one of the fastest growing renewable energy sources (DOE 2008). Modern

wind turbines are large, flexible structures operating in uncertain environments. Because larger wind turbines have power capture and economical advantages, the typical size of utility-scale wind turbines has increased substantially over the last three decades (Quarton 1998; DOE 2008). This increase in scale has led to increased loads on wind turbine structures. This, combined with uncertain conditions and demand (among other factors), has resulted in many unsolved challenges associated with improving the quality, reliability, and economical competitiveness of wind energy extraction. Many of these challenges are connected to the interface of mechanical and control system design for wind energy systems. A large body of work exists that is devoted to maximizing energy extraction through optimal control system design (in particular, rotor speed control and/or blade pitch control). Engineers have also studied optimal wind turbine physical (plant) design. These two aspects of wind turbine design (plant and control) are closely interrelated, but so far have largely been treated as independent activities. The conventional sequential approach of plant design followed by control design will not yield system-optimal results.

This article presents an integrated approach to achieve system optimal wind turbine designs through combined plant and control co-design, accounting for the synergistic coupling between mechanical and control system aspects of horizontal axis wind turbine (HAWT) design. A comparison is also provided between co-design and conventional sequential design of HAWTs.

The paper is structured as follows. Section 2 introduces the performance characteristics of the HAWTs and reviews the relevant literature. This is followed by an explication of co-design formulations in Section 3. The co-design problem for wind turbines is then introduced in Section 4, and results and discussion are presented in Section 5.

2 Performance characteristics of HAWT and previous work

Consider the model for wind turbine rotor power, P_w, given by:

$$P_w(v) = \frac{1}{2} C_P(\lambda, \beta) \rho \pi {R_r}^2 v^3 \tag{1}$$

where $C_p(\cdot)$ is the power coefficient. $C_p(\cdot)$ is a nonlinear function of blade tip speed ratio λ (the ratio of blade tip speed and wind speed: $\lambda = R_r \Omega_r / v$) and blade pitch angle β. The air density is ρ, R_r is the rotor radius, Ω_r is the rotor speed and v is the wind speed (assumed here to be uniform over the entire swept rotor area). For a given physical turbine design and wind speed, the power capture maximization problem reduces to tracking the optimal power coefficient ($C_{p_{\text{opt}}}$), by controlling the blade-tip speed ratio (via generator torque) and blade pitch angle. As shown in Fig. 1, for each wind speed there exists a point on the HAWT rotor torque-speed map that corresponds to the optimal power coefficient.

The operating regimes for wind turbine systems have traditionally been categorized into three operational zones (ref. Fig. 2), Zone 1: below cut-in wind speed (i.e., speeds below the minimum required to produce useful power), Zone 2: between cut-in and rated wind speeds, Zone 3: between rated and cut-out speed (cut-out speed is the speed at which turbine operation must be modified to prevent damage), and Zone 4: above the cut-out wind speed. Wind turbines are often shut-down in Zone 4 to prevent damage due excessive wind loads. A range of performance objectives can be identified that apply to one or more of these zones:

1. Maintaining the wind power at rated for speeds greater than rated (Zone 3);
2. Maximizing the wind harvested energy in the partial load zone as long as constraints on speed and captured power are met (Zone 2);
3. Ameliorating load variability to improve mechanical and structural system resilience (Zones 2 and 3);
4. Meeting strict power quality standards (power factor, harmonics, flicker, etc.) (Zones 2 and 3);
5. Transferring the electrical power to the grid at an imposed level across a wide range of wind velocities (Zone 3).

When designing the wind turbine for maximum energy production (objective 2 above), an important metric to consider is Annualized Energy Production (AEP). AEP accounts for the variability in the wind over time by considering the wind speed probability distribution at a particular site. AEP can be interpreted as the expected annualized energy output from a wind turbine for a given wind speed distribution and a HAWT design. This wind speed distribution can be modeled using one of two distributions that are

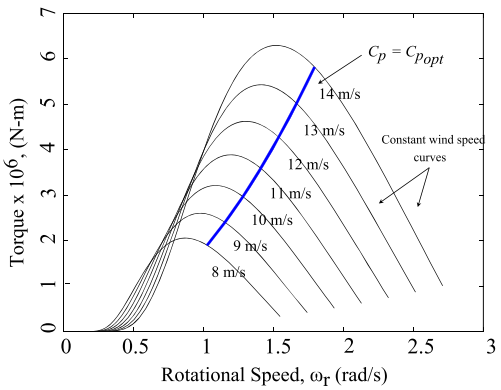

Fig. 1 Maximum power coefficient ($C_{p_{\text{opt}}}$) tracking

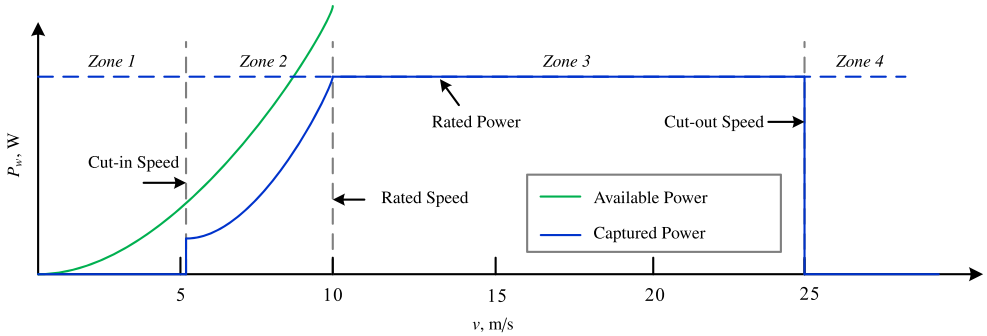

Fig. 2 Different operating zones of a wind turbine

considered to be most appropriate for wind speed: Rayleigh distribution or Weibull distribution (He et al. 2010). In the work presented here, a two parameter Weibull distribution was used:

$$p(v) = \frac{k}{c}\left(\frac{v}{c}\right)^{k-1} e^{-(\frac{v}{c})^k} \tag{2}$$

where v is the wind speed and k and c are Weibull parameters. Based on this distribution, the Annualized Energy Production (AEP), in Wh/yr, can be quantified as:

$$AEP = 8760 \times \int_{v_i}^{v_o} P_w(v)\frac{k}{c}\left(\frac{v}{c}\right)^{k-1} e^{-(\frac{v}{c})^k} dv \tag{3}$$

where v_o is the cut-out speed, v_i is the cut–in speed, and 8760 is the total number of hours in a 365 day calendar year. Figure 3 illustrates AEP contours for a particular wind turbine as a function of rotor diameter. This chart indicates the achievable AEP for a wind turbine of a particular power rating operating at certain capacity factor. The capacity factor of a wind turbine is the ratio of actual output over a period of time to maximum potential output (i.e., if the turbine could operate at full rated capacity indefinitely). Rated power is the nameplate maximum power capacity of the wind turbine.

Please note that two distinct types of wind energy system design problems are addressed often in the design literature: 1) individual wind turbine optimization, and 2) wind farm layout optimization (e.g., Chowdhury et al. 2010, 2012, 2013a, b; DuPont and Cagan 2012; Chen and MacDonald 2012, 2014; Lu and Kim 2014). The scope of this article is limited to individual wind turbine design optimization. The following subsections will review individual wind turbine optimization studies in the existing literature.

2.1 Wind turbine structural design

Optimal structural design for wind turbines is traditionally concerned with the design of rotor (including blades) and tower. A significant body of research can be found on blade design for improved efficiency and energy capture (Giguere et al. 1999; Benini and Toffolo 2002; Jureczko et al. 2005). Studies pertaining to optimal tower design include tower mass minimization (Yoshida 2006; Nicholson 2011), vibration reduction (Uys et al. 2007) and stiffness maximization (Negm and Maalawi 2000).

Tower mass correlates strongly with structural system cost. Mass and cost reduction competes with the need to construct taller towers to improve energy capture. Increasing height while targeting lower mass designs results in lighter-weight towers with significant elastic compliance. This increased compliance intensifies the risk of aeroelastic instabilities, adding to design and reliability challenges, and hindering efforts to improve energy capture (Holley 2003). The coupling between structural dynamics and control of the turbine and generator, which is stronger for taller more compliant towers, motivates the investigation and use of integrated design approaches that address structural and control system design simultaneously to account for (an even capitalize on) control-structure interaction.

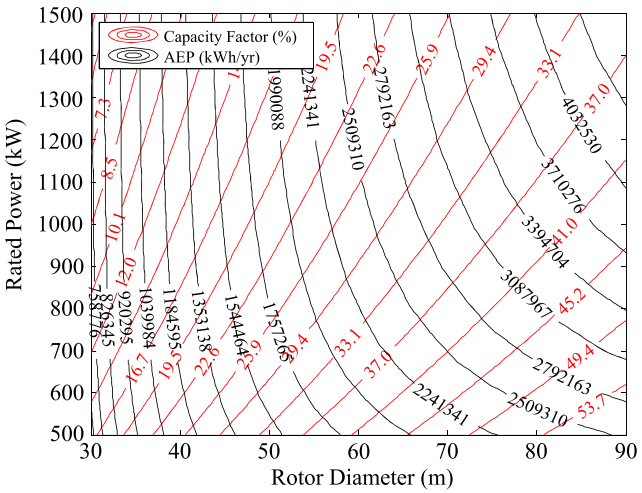

Fig. 3 AEP contours for a particular wind distribution for Weibull parameters: $k = 1.91$, $c = 6.80$, $v_{mean} = 6.03\ m/s$, generated using HARP–Opt tool (Sale 2010)

2.2 Optimal control for wind turbines

The key concept behind energy maximization via optimal control is to ensure that optimal power production is maintained at each time step for current wind conditions. Based on the model presented in (1), this is achieved by maintaining a maximum power coefficient ($C_{p_{\text{opt}}}$) for all wind speeds in Zone 2. This can be viewed as a control problem in which blade pitch angle (β) and rotor speed (Ω_r, in turn affecting λ) are controlled to maintain desired C_p. The blade pitch control modifies the performance of the system by affecting rotor aerodynamics directly. Rotor speed can be controlled indirectly via generator control, and can be varied to achieve $C_{p_{\text{opt}}}$ as shown in Fig. 1. In addition, there exists a power conditioning control system that operates on the grid connection subsystem to smooth out fluctuations in generated power. These control subsystems are depicted in Fig. 4. This investigation focuses primarily on variable rotor speed control.

Many types of variable speed control have been presented in the literature. Thiringer and Linders (1993) performed an early investigation of power capture maximization via rotor speed control in a variable-speed, fixed-pitch machine configuration. The variable speed control works by modulating the generator speed (and hence the rotor speed) based on the input wind speed to the turbine. Unfortunately, accurate measurement of instantaneous wind speed is difficult. One sensing strategy involves placing an anemometer on top of the nacelle. This location is downstream of the blade, so the wind speed ahead of the rotor can not be measured accurately at this location. Successful $C_{p_{\text{opt}}}$ tracking requires better estimates of free stream wind speed.

Another strategy for measuring the wind speed in front of the rotor accurately, ahead of time, is to use light detection and ranging (LIDAR) (Scholbrock et al. 2013). This method is fairly successful for rotor speed control when wind speed variation is gradual, but its accuracy suffers under turbulent wind conditions. Another alternative called maximum power point tracking (MPPT) does not rely on wind speed prediction (Munteanu et al. 2008, pp. 76–77). In this approach the rotor speed reference is modified by a variation $\Delta\Omega_r$ that is based solely on a corresponding change in power P_w. The sign of $\frac{\partial P_w}{\partial \Omega_r}$ indicates the position of the operating point with respect to the maximum of $P_w(\Omega_r)$. The rotor speed reference is adjusted linearly with a rate proportional to this derivative, with a hope that the system evolves to optimum, where $\frac{\partial P_w}{\partial \Omega_r} = 0$. While this method is easier to implement, it is known to result in significant load fluctuations, shortening component lives. Most previous efforts reported in the literature have been focused on individual wind turbine design disciplines or objectives, such as optimal control for power production, control for load alleviation, or structural design (Maalawi and Negm 2002; Xudong et al. 2009; Soltani et al. 2011),

Model Predictive Control (MPC) is another promising approach for optimizing systems with slowly varying dynamics. MPC is very convenient for systems with actuator and path constraints. It has been extended to wind power maximization (Dang et al. 2009, 2010; Burnham 2009; Kusiak et al. 2010). Faster versions of MPC (Wan and Kothare 2003; Wang and Boyd 2010) have also been proposed recently that can be applied to systems with fast varying dynamics.

The above studies focus on rotor speed or torque control. An alternative strategy is to control blade pitch (Stotsky and Egardt 2013; Boukhezzar et al. 2007; Muljadi and Butterfield 2001). For example, Namik and Stol (2011) proposed a method based on individual blade pitch control that improved power output performance for onshore and offshore wind turbines. They showed that using individualized blade pitch control enhances wind disturbance rejection, helps reduce structural tower loads, and improves power capture.

2.3 Multidisciplinary design optimization of wind turbines

Optimizing engineering systems with respect to just one discipline (e.g. structures, aerodynamics, control systems, etc.) does not produce the best possible system performance when interdisciplinary interactions are present. This phenomenon has been well-studied by the multidisciplinary design optimization (MDO) research community,

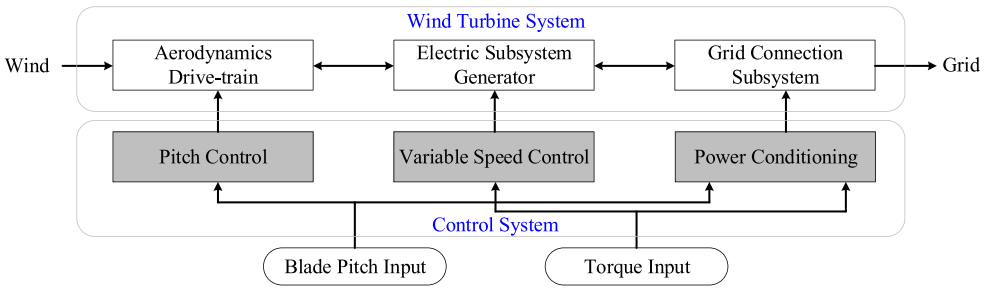

Fig. 4 Main control subsystems of wind turbine

and numerous MDO design methodologies have been developed that account for multidisciplinary design coupling (Cramer et al. 1993; Sobieszczanski-Sobieski and Haftka 1997; Martins and Lambe 2013). HAWTs are good examples of multidisciplinary systems; aerodynamic loads produce structural blade and tower deflections, and structural deflections influence aerodynamic loads. These aeroelastic effects are further coupled with generator dynamics and control system effects. Several recent studies have utilized MDO for wind turbine design (Zakhama and Abdalla 2010; Forcier and Joncas 2012). For example, Ashuri et al. (2014) optimized the rotor and tower simultaneously, including satisfaction of relevant aerodynamic and structural constraints. This study also identified the need to include controller parameters as a part of the design optimization process to reduce the levelized cost of energy (LCOE). Accounting for the interaction between aeroelasticity and control system design is an emerging area of HAWT research, and is a primary focus of this article.

2.4 Co-design as MDO

Addressing either control system or plant design alone without considering the potential synergy between these domains will not lead to the best possible system performance. In practice, control systems often are designed after physical system design is complete (i.e., sequential design), with limited interaction between mechanical and control system engineers. Whether in research or practice, plant and control design decisions should be made simultaneously to support exploration of true system performance limits. Integrated design methods, often termed co-design methods, are being developed that produce system-optimal designs by accounting fully for the coupling between plant and control system design (Fathy et al. 2001; Allison 2013; Allison and Herber 2014; Allison et al. 2014).

In the context of wind turbine system design, there is a strong need to solve multidisciplinary design optimization problems involving integrated aero–servo–hydro–elastic analyses, as identified by Jonkman (2009), to obtain system-optimal designs. Significant advancements in wind energy system performance and economic competitiveness require design methods with tighter integration between physical system (plant) and control system design at a much earlier phase in design process. Co-design is an important strategy for investigating and understanding mechatronic system performance limits, and is a practical means for exploiting synergistic relationships to improve performance. Co-design may also be viewed as a special case of MDO, where one of the coupled disciplines is control system design, and physical system design is addressed using one or more disciplines (see Allison et al. (2014) for a comparison of several MDO and co-design formulations). The following section details the co-design formulations that are relevant to the HAWT investigation presented here.

3 System co-design

Co–design is a class of design optimization methods for actively-controlled dynamic systems. Design of physical systems and their associated control systems are often coupled tasks; design methods that manage this interaction explicitly can produce system-optimal designs, whereas conventional sequential processes (i.e., plant design followed by control design) may not (Reyer et al. 2001). In this section, we review the sequential design process, followed by a discussion of two co–design formulations: nested and simultaneous.

3.1 Sequential system design

In design practice, the sequential design approach is used most often when developing actively controlled engineering systems. This involves designing the physical system first, and then designing the control system without modifying the plant design. When optimization is used, the sequential approach produces optimal solutions with respect to individual disciplines, plant and control design, but normally will not produce a system-optimal solution. Sequential design strategies do not account fully for plant-control design coupling, so are not considered to be co-design methods. The mathematical formulation for sequential system design includes both the plant and control design optimization problems. Here the plant design optimization problem is formulated as follows:

$$\begin{aligned} \min_{\mathbf{x_p}} \quad & \phi(\boldsymbol{\xi}(t), \mathbf{x_p}) \\ \text{subject to:} \quad & \mathbf{g_p}(\boldsymbol{\xi}(t), \mathbf{x_p}) \leq \mathbf{0} \\ \text{where:} \quad & \dot{\boldsymbol{\xi}}(t) - \mathbf{f}(\boldsymbol{\xi}(t), \mathbf{x_p}) = \mathbf{0}. \end{aligned} \tag{4}$$

where, $\mathbf{x_p}$ is the vector of plant design variables, $\phi(\cdot)$ is the plant design objective, $\mathbf{g_p}(\cdot)$ is the vector of plant constraint functions, $\boldsymbol{\xi}(t)$ are time dependent system states, and $\mathbf{f}(\cdot)$ represents the passive system dynamics that need to be satisfied by the states $\boldsymbol{\xi}(t)$. The solution to Prob. (4)—i.e., the optimal plant design vector $\mathbf{x_{p_*}}$—is used as the basis for the optimal control design problem. The objective and constraint functions in the optimal control problem depend on $\mathbf{x_{p_*}}$, but its value is held fixed during the solution of optimal control problem:

$$\begin{aligned} \min_{\mathbf{x_c}} \quad & \phi(\boldsymbol{\xi}(t), \mathbf{x_c}, \mathbf{x_{p_*}}) \\ \text{subject to:} \quad & \mathbf{g_p}(\boldsymbol{\xi}(t), \mathbf{x_{p_*}}) \leq \mathbf{0} \\ \text{where:} \quad & \dot{\boldsymbol{\xi}}(t) - \mathbf{f}(\boldsymbol{\xi}(t), \mathbf{x_c}, \mathbf{x_{p_*}}) = \mathbf{0}. \end{aligned} \tag{5}$$

where, $\mathbf{x_c}$ is used here to represent control system design variables in a general way. These variables could take the form of a set of feedback gain variables for a given control system architecture, or the form of function-valued control input trajectories $\mathbf{u}(t)$.

The sequential design problem may be formulated in several ways; the problems above illustrate one possible formulation. One important difference between formulation strategies is the nature of the objective function used in each problem. Allison and Herber (2014) presented a taxonomy of sequential design formulations; the plant design formulation here is Type 1 under this taxonomy. More specifically the plant design objective accounts only for passive plant dynamics, but is based on the overall system design objective function. In much of the literature a distinct objective function is formulated for the plant design problem. In many previous design studies, the plant and control design objectives are treated as distinct, forming a multi-objective optimization problem. In most of these cases, however, the plant design objective is actually a simplified approximation of the control design objective, adjusted to be congruent with design paradigms that are embraced by mechanical or structural design engineers. These proxy plant objectives are often static or pseudo-static performance metrics that do not account fully for system dynamics.

3.2 Co-design formulation and solution fundamentals

The formulation presented here involves a single system objective function that is used consistently across both plant and control design domains. Here we assume that this objective function depends on control and state trajectories, e.g., it is of the form $\phi(\cdot) = \int_{t_0}^{t_F} L(\boldsymbol{\xi}(t), \mathbf{x_c}, \mathbf{x_p})dt$, where $L(\cdot)$ is a Lagrangian function, and t_0 and t_F define the time horizon of interest. System optimality requires that a consistent system design objective is applied across both plant and control design domains. It may be that the system design problem is inherently multi-objective; if this is the case, then all system objectives should be applied consistently across plant and control design problems.

In more complete co-design formulations, the plant design depends on state. For example, stress values in a turbine tower or blades depend on structural vibrations that are characterized by system state. While both the objective function and constraints will depend directly on state, only the objective function will depend directly on control design. Plant constraints, however, will depend indirectly on control design since state trajectories are influenced by control design. From these observations it can be concluded that many co-design problems exhibit bi-directional coupling; i.e., plant design depends on control design, and vice versa. One important consequence of plant constraints dependance on state is the need to include plant constraints in the control optimization problem. If plant constraints that depend on state are omitted from control optimization formulations, a feasible system design may be impossible to identify.

Several options exist for solving the optimal control problem. A classical or 'indirect' approach is to apply optimality conditions—such as Pontryagin's Maximum Principle (PMP) (Pontryagin 1962; Bryson and Ho 1975)—and then solve for the optimal control trajectory $\mathbf{u}_*(t)$ that minimizes $\phi(\cdot)$. Application of optimality conditions produces a two–point boundary value problem (TPBVP). In some cases this problem can be solved analytically to produce a closed-form solution, but this is only possible in simpler cases. If a closed-form solution cannot be obtained, the TPBVP often can be solved numerically. This approach is therefore known as an 'optimize–then–discretize' approach, since optimality conditions are applied first to obtain a BVP, which is then discretized and solved (Biegler 2010). One significant challenge in utilizing indirect optimal control methods in co-design is the need to satisfy inequality plant constraints. This is not possible in the general case. In addition, when plant design is part of an optimization problem, it can be difficult to obtain the derivatives needed to form and solve the TPBVP. Other optimization methods are needed that are more naturally suited for solving co-design problems.

Optimal control problems may also be solved using direct methods, where an infinite-dimensional optimal control problem, such as the one given in Prob. (5), is 'transcribed directly' into a finite-dimensional nonlinear program (NLP). The discretized optimization problem can then be solved numerically using appropriate NLP algorithms, and can accommodate inequality plant constraints and plant design variables easily. This optimal control approach, known as Direct Transcription (DT) (Biegler 2010; Betts 2010), is classified as a 'discretize–then–optimize' method, since discretization is performed before optimization. It was first applied to co-design problems by Allison et al. (2014).

3.2.1 Nested co–design

Allison and Herber (2014) identified the nested co-design formulation as a special case of the Multidisciplinary Design Feasible (MDF) formulation. This formulation has two loops: an outer loop that solves the plant design optimization problem, and an inner loop generates the optimal control for each plant design considered by the outer loop. The outer loop formulation is:

$$\begin{aligned} \min_{\mathbf{x_p}} \quad & \phi_*(\mathbf{x_p}) \\ \text{subject to:} \quad & \mathbf{g_p}(\mathbf{x_p}) \leq \mathbf{0}, \end{aligned} \tag{6}$$

where $\mathbf{x_p}$ is the plant design vector, $\mathbf{g_p}(\cdot)$ are the plant design constraints, and $\phi_*(\cdot)$ is an optimal value function that depends only on $\mathbf{x_p}$. This optimal value function is evaluated by solving the inner loop optimal control problem, i.e., for a given plant design, it finds the optimal control and returns the objective function value. Note that the same objective function is used for both the inner and outer loops; the difference is that for every objective function evaluation in the outer loop, the optimal control for the candidate plant design is found and held fixed. More specifically, for every outer loop function evaluation, the inner loop is solved for the optimal control design vector $\mathbf{x_{c*}}$:

$$\begin{aligned} \min_{\mathbf{x_c}} \quad & \phi(\boldsymbol{\xi}(t), \mathbf{x_c}, \mathbf{x_p}) \\ \text{subject to:} \quad & \mathbf{g_p}(\boldsymbol{\xi}(t), \mathbf{x_p}) \leq \mathbf{0} \\ \text{where:} \quad & \dot{\boldsymbol{\xi}}(t) - \mathbf{f}(\boldsymbol{\xi}(t), \mathbf{x_c}, \mathbf{x_p}) = \mathbf{0}. \end{aligned} \tag{7}$$

As can be seen from above formulation, the plant design is held fixed during the inner loop solution. Plant design constraints $\mathbf{g_p}(\cdot)$ are imposed in both loops to ensure system-level design feasibility. As with sequential system design, the optimal control problem must be solved using an optimization method that can accommodate inequality plant design constraints.

3.2.2 Simultaneous co-design

The simultaneous co-design problem formulation is:

$$\begin{aligned} \min_{\mathbf{x_p}, \mathbf{x_c}} \quad & \phi(\boldsymbol{\xi}(t), \mathbf{x_c}, \mathbf{x_p}) \\ \text{subject to:} \quad & \mathbf{g_p}(\boldsymbol{\xi}(t), \mathbf{x_p}) \leq \mathbf{0} \\ \text{where:} \quad & \dot{\boldsymbol{\xi}}(t) - \mathbf{f}(\boldsymbol{\xi}(t), \mathbf{x_c}, \mathbf{x_p}) = \mathbf{0}. \end{aligned} \tag{8}$$

The solution to Prob. (8) yields the system-optimal design because it accounts for all dynamic system interactions and plant-control design coupling, resulting in a minimum $\phi(\cdot)$ that is lower than what could be achieved using the sequential approach. This formulation is often referred to as the simultaneous co-design method, as plant and control design decisions are made simultaneously. Mathematical equivalence can be demonstrated between the simultaneous and nested co-design formulations, as long as the objective functions are the same (Fathy et al. 2001) and plant constraints are satisfied in the inner loop of the nested problem (Allison and Herber 2014).

3.3 Direct transcription

Conventional optimal control methods based on Pontryagin's Maximum Principle (1962) take an 'optimize–then–discretize' approach, where optimality conditions are applied to generate a closed–form solution (possible only in limited cases), or a boundary value problem that can then be discretized and solved for the optimal control trajectories. Direct Transcription (DT) takes the inverse approach: the optimal control problem is discretized first, and the resulting nonlinear program (NLP) is solved using a standard NLP algorithm (Betts 2010; Biegler 2010). DT is a 'discretize–then–optimize' approach that transcribes an infinite–dimensional optimal control problem into a large sparse finite dimensional NLP. State and control trajectories trajectories are discretized over a finite number of time intervals, and these discretized trajectory representations are part of the set of optimization variables. The differential constraint that governs system dynamics is replaced by a finite set of algebraic defect constraints. These defect constraints can be formed using any standard numerical collocation method, such as implicit Runge-Kutta (IRK) methods or Gaussian quadrature. The trapezoidal method, an IRK method, is used in the implementations here. Allison et al. (2014) introduced an extension of DT for co-design problems, including an analysis of changes in problem structure. A DT co-design formulation based on this work, using the trapezoidal collocation method, follows:

$$\begin{aligned} \min_{\mathbf{y}=\mathbf{x_p}, \boldsymbol{\Xi}, \mathbf{U}} \quad & \sum_{i=1}^{n_t-1} L(\mathbf{x_p}, \boldsymbol{\xi}_i, \mathbf{u}_i) h_i \\ \text{subject to:} \quad & \boldsymbol{\zeta}(\mathbf{x_p}, \mathbf{U}, \boldsymbol{\Xi}) = \mathbf{0} \\ & \mathbf{g_p}(\mathbf{x_p}, \boldsymbol{\Xi}) \leq \mathbf{0}. \end{aligned} \tag{9}$$

where n_t is the number of steps in the time discretization, $\boldsymbol{\Xi} = [\boldsymbol{\xi}_1, \ \boldsymbol{\xi}_2, \ \cdots \ \boldsymbol{\xi}_{n_t}]^{\mathrm{T}}$ is the matrix of discretized state variables (row i corresponds to the state at time t_i), $\boldsymbol{\zeta}(\cdot)$ are the defect constraint functions imposed to ensure that $\boldsymbol{\Xi}$ satisfies system state equations, $\mathbf{U} = [\mathbf{u}_1, \ \mathbf{u}_2, \ \cdots, \ \mathbf{u}_n]^{\mathrm{T}}$ is control input matrix, and h_i is the i^{th} time step size. The summation is a discretized approximation of the integral system objective function made using a simple quadrature method. The NLP in Prob. (9) can be solved using standard gradient based optimization algorithms. An important advantage of DT to emphasize here is its parallel nature; all defect constraints are independent, enabling massively parallel implementations. With background in co-design and DT established, the subsequent sections will discuss the wind turbine co-design problem and results.

4 Wind turbine co–design

The design of a wind turbine system in conceptual stages is fundamentally multidisciplinary, requiring consideration of the structural design of tower, blades and drive-train, as well as blade aerodynamic design. Traditionally, the structural and aerodynamic design is done in tandem over multiple iterations between the corresponding teams. However, the

control system design has always been performed after the physical plant design is completed. As pointed out in earlier sections, this sequential design strategy results in suboptimal system designs. To improve system performance and economic competitiveness, we propose the use of a novel co–design formulation that is truly multidisciplinary in nature, considering aero–servo–elastic interactions throughout the design solution process. The end goal of this design optimization is to find the optimal plant geometry and open-loop control strategy that maximizes AEP.

4.1 System design formulation

As a first step, consider the problem of maximizing AEP only with respect to plant design. Later we will introduce an optimal control formulation, and then an integrated co-design problem formulation. The objective in the plant design optimization problem is to maximize the AEP while satisfying plant constraints by choosing the appropriate blade and tower geometry.

$$\begin{aligned} \max_{\mathbf{x_p}} \quad & AEP(v(t), P_w(v)) \\ \text{subject to:} \quad & \mathbf{A_g x_p} \leq \mathbf{0} \\ & \mathbf{g_p}(\boldsymbol{\xi}(t), \mathbf{x_p}) \leq \mathbf{0} \\ & \mathbf{0} < \mathbf{x_l} \leq \mathbf{x_p} \leq \mathbf{x_u} \\ \text{where:} \quad & \dot{\boldsymbol{\xi}}(t) - \mathbf{f}(\boldsymbol{\xi}(t), \mathbf{x_p}) = \mathbf{0} \end{aligned} \tag{10}$$

where $\mathbf{x_p}$ is the plant design vector and $AEP(\cdot)$ expression is as defined in (3). The $AEP(\cdot)$ here implicitly depends on $\mathbf{x_p}$ through the power P_w (1). Finally, $\boldsymbol{\xi}(t)$ are the system state trajectories that satisfy the the differential equation $\dot{\boldsymbol{\xi}}(t) - \mathbf{f}(\boldsymbol{\xi}(t), \mathbf{x_p}) = \mathbf{0}$ which models the dynamics of the wind turbine system, consisting of multiple bodies.

These multi-body dynamic equations are implemented in FAST, a software tool developed by the National Renewable Energy Laboratory (NREL) for evaluating aeroelastic wind turbine behavior (Jonkman and Buhl 2004). FAST relies internally on AeroDyn, an aerodynamic analysis module that predicts aerodynamics loads acting on turbine blades due to incoming wind using Blade Element Theory (Moriarty and Hansen 2005). These loads are then utilized within FAST for multi-body dynamic analysis.

The derivation of the equations used in FAST is based on the standard Kane's system of equations approach (Bajodah 2005):

$$\mathbf{C}(\mathbf{q}, t)\ddot{\mathbf{q}} + \mathbf{f}(\dot{\mathbf{q}}, \mathbf{q}, t) = \mathbf{0}. \tag{11}$$

After rearranging the terms in (11) and defining $\boldsymbol{\xi} = [\mathbf{q} \;\; \dot{\mathbf{q}}]^T$ as the state vector, we can write the system dynamics in the form: $\dot{\boldsymbol{\xi}}(t) - \mathbf{f}(\boldsymbol{\xi}(t), \mathbf{x_p}) = \mathbf{0}$. Table 1 defines the first four states, q_i. These states correspond to a simplified set of mechanical degrees of freedom chosen for this case study. The remaining four states are the time derivatives of first four.

The physical design vector $\mathbf{x_p}$ is defined as:

$$\mathbf{x_p} = [t_{w1},\ t_{w2},\ t_{w3},\ t_{w4},\ t_{w5},\ c_1,\ c_2,\ c_3,\ c_4,\ c_5,\ t_{h1},\ t_{h2},\ t_{h3},\ D_h,\ D_r,\ H_t]^T$$

The individual elements of $\mathbf{x_p}$ are defined as in Table 2.

The linear inequality constraints on $\mathbf{x_p}$ are defined by the relation $\mathbf{A_g x_p} \leq \mathbf{0}$. These linear constraints maintain a non-increasing blade pre-twist angle, chord length, and thickness along the blade span. The last row of $\mathbf{A_g}$ is defined to ensure that the rotor radius is smaller than the tower height at the hub (ensuring no interference between blades and ground). The lower and upper bounds on the plant design vector $\mathbf{x_p}$ are $\mathbf{x_l}$ and $\mathbf{x_u}$, respectively.

$$\mathbf{A_g} = \begin{bmatrix} -1 & 1 & 0 & 0 & 0 & 0 & 0 & 0 & 0 & 0 & 0 & 0 & 0 & 0 & 0 & 0 \\ 0 & -1 & 1 & 0 & 0 & 0 & 0 & 0 & 0 & 0 & 0 & 0 & 0 & 0 & 0 & 0 \\ 0 & 0 & -1 & 1 & 0 & 0 & 0 & 0 & 0 & 0 & 0 & 0 & 0 & 0 & 0 & 0 \\ 0 & 0 & 0 & -1 & 1 & 0 & 0 & 0 & 0 & 0 & 0 & 0 & 0 & 0 & 0 & 0 \\ 0 & 0 & 0 & 0 & 0 & -1 & 1 & 0 & 0 & 0 & 0 & 0 & 0 & 0 & 0 & 0 \\ 0 & 0 & 0 & 0 & 0 & 0 & -1 & 1 & 0 & 0 & 0 & 0 & 0 & 0 & 0 & 0 \\ 0 & 0 & 0 & 0 & 0 & 0 & 0 & -1 & 1 & 0 & 0 & 0 & 0 & 0 & 0 & 0 \\ 0 & 0 & 0 & 0 & 0 & 0 & 0 & 0 & -1 & 1 & 0 & 0 & 0 & 0 & 0 & 0 \\ 0 & 0 & 0 & 0 & 0 & 0 & 0 & 0 & 0 & 0 & 1 & -1 & 0 & 0 & 0 & 0 \\ 0 & 0 & 0 & 0 & 0 & 0 & 0 & 0 & 0 & 0 & 0 & 1 & -1 & 0 & 0 & 0 \\ 0 & 0 & 0 & 0 & 0 & 0 & 0 & 0 & 0 & 0 & 0 & 0 & 1 & -1 & 0 & 0 \\ 0 & 0 & 0 & 0 & 0 & 0 & 0 & 0 & 0 & 0 & 0 & 0 & 0 & \frac{1}{2} & -1 & 0 \end{bmatrix}$$

The nonlinear plant inequality constraints $\mathbf{g_p}(\cdot) \leq \mathbf{0}$ enforce limits on stress, strain, and natural frequencies. Some of the specific constraints in $\mathbf{g_p}(\cdot)$ include limits on the mean stress at the base of the tower, as well as limits on stresses and strains at the blade leading and trailing edges. It should be noted here that these constraints depend both on plant design vector as well as system states (and hence indirectly on control design).

4.2 Blade geometry design

As detailed in Table 1, three elements of blade geometry are defined: blade pre-twist distribution along the span, chord distribution along the span, and thickness along the span (Sale 2010). Each of these geometric elements is a function-valued quantity (value depends on position along the blade span). These functions are represented using Bézier curves (Zeid 1991), which are each parameterized using several control points. These control points are used as the plant design variables for blade geometry. The Bézier curve for $n+1$ control points can be defined mathematically as:

$$\mathbf{C}(p) = \sum_{i=0}^{n} \mathbf{P}_i B_{i,n}(p) \tag{12}$$

Table 1 HAWT plant design vector description

Variable	Description
t_{wi}	i^{th} control point for blade pre–twist angle along the blade span, for $i = 1, 2 \ \ldots \ 5$.
c_i	i^{th} control point for chord length along the blade span, for $i = 1, 2 \ \ldots \ 5$.
t_{hi}	i^{th} control point for thickness along the blade span, for $i = 1, 2, 3$.
D_h	Hub diameter of the wind turbine blade
D_r	Rotor diameter of the wind turbine
H_t	Tower height at the hub.

where, $p \in [0, 1]$, $\mathbf{P}_i$'s are the control points, and $B_{i,n}(p)$ is a Bernstein polynomial:

$$B_{i,n}(p) = \frac{n!}{i!(n-i)!} p^i (1-p)^{n-i}, \quad i = 1, 2, \ \ldots \ n \quad (13)$$

In addition to these control points, three control points for the blade circular root are also defined. These control points are necessary to ensure a circular shape of the blade root where the blade connects to the rotor hub. The blade geometry is divided into 30 segments along the blade span for aerodynamic analysis and blade performance evaluation, providing moderate-fidelity analysis.

4.3 Optimal control

This subsection defines the problem of optimizing system performance with respect to control design only. Here variable rotor speed control is used (cf. Fig. 4); blade pitch is assumed to be fixed. The optimal control problem is to maximize AEP with respect to the generator torque trajectory $\Gamma_g(t)$ over a given finite time horizon ($0 \le t \le t_f$), subject to differential and algebraic constraints. Adjusting generator inputs can control generator torque, which in turn influences rotor speed. The optimal control formulation is:

$$\begin{aligned} \max_{\mathbf{u}(t)=\Gamma_g(t)} \quad & AEP(v(t), P_w(v)) \\ \text{subject to:} \quad & \mathbf{g_p}(\boldsymbol{\xi}(t), \mathbf{x}_{\mathbf{p}_*}) \le \mathbf{0} \\ & \|\lambda(\Omega_r(t), v(t)) - \lambda_{\text{opt}}(\Omega_r(t), v(t))\| = 0. \\ \text{where:} \quad & \dot{\boldsymbol{\xi}}(t) = \mathbf{f}(\boldsymbol{\xi}(t), \mathbf{x_p}, \mathbf{u}(t)) \end{aligned} \quad (14)$$

where $\lambda(\cdot) = \Omega_r(t) R_r / v(t)$ is the instantaneous tip–speed ratio, and R_r is the blade length. The $AEP(\cdot)$ here depends on P_w (1), which in turn depends on $C_P(\cdot)$ that is affected by the control $\mathbf{u}(t)$. In other words, $AEP(\cdot)$ depends on $\mathbf{u}(t)$. From (10) and (14), the dependence of $AEP(\cdot)$ on both $\mathbf{x_p}$ and $\mathbf{u}(t)$ is clear.

The solution of problem (14) is the open-loop optimal control strategy. The second constraint above ($\|\cdot\| = 0$, where $\|\cdot\|$ is an l_2 norm) ensures that the actual tip-speed ratio $\lambda(t)$ matches the steady-state optimal tip–speed ratio $\lambda_{\text{opt}}(t)$ over the full time horizon, resulting in attainment of steady-state optimal power coefficient $C_{p_{\text{opt}}}(t)$. In other words, this constraint is satisfied if a generator torque trajectory $\Gamma_g(t)$ (the control input) is found that results in a rotor speed $\Omega_r(t)$, that matches the optimal reference speed defined by $\lambda_{\text{opt}}(t)$.

This can be better understood by looking at the drive-train dynamics which constitute a crucial part of overall system dynamics: $\dot{\boldsymbol{\xi}}(t) = \mathbf{f}(\cdot)$. Assuming a perfectly rigid drive-train, we can write the single mass dynamic model (Boukhezzar et al. 2007; Jonkman and Buhl 2005) as: .

$$\begin{aligned} J_t \dot{\Omega}_r(t) &= \Gamma_r(t) - B_t \Omega_r(t) - \eta \Gamma_g(t) \\ \text{where:} \quad J_t &= J_r + \eta^2 J_g \\ B_t &= B_r + \eta^2 B_g \end{aligned} \quad (15)$$

where, η is the drive-train gear ratio, Ω_r is the rotor speed, J_r, J_g, B_r and B_g are the rotor inertia, generator inertia, rotor damping, and generator damping values, respectively. Wind flowing across the blades produces a torque on the rotor $\Gamma_r(\cdot)$. This is resisted by the generator torque $\Gamma_g(\cdot)$. The torque due to wind is:

$$\Gamma_r(t) = \frac{1}{2} C_Q(\lambda, \beta) \rho \pi {R_r}^3 v^2$$

where $C_Q(\lambda, \beta) = \frac{C_P(\lambda, \beta)}{\lambda}$ is the torque coefficient. The difference between rotor and generator torque (accounting for the drive-train ratio η), results in angular acceleration

Table 2 Description of first 4 system states

State	Description
q_1	Drive–train torsional compliance DOF
q_2	Generator DOF
q_3	First fore-aft tower bending-mode DOF
q_4	First side–to–side tower bending–mode DOF

or deceleration of the rotor, subject to damping B_t in the drive-train system.

4.4 Co-design formulations

The individual plant and control design problems are defined above, and now two different co-design formulations can be introduced: nested and simultaneous.

Nested formulation The outer-loop problem of nested formulation is:

$$\begin{aligned} \max_{\mathbf{x_p}} \quad & AEP_*(v(t), P_w(v)) \\ \text{s.t.:} \quad & \mathbf{A_g x_p} \leq \mathbf{0} \\ & \mathbf{g_p}(\mathbf{x_p}) \leq \mathbf{0} \\ & \mathbf{0} < \mathbf{x_l} \leq \mathbf{x_p} \leq \mathbf{x_u}, \end{aligned} \tag{16}$$

For each candidate plant design $\mathbf{x_p}$ considered during the outer-loop solution process, the inner-loop problem is solved to identify the optimal control trajectory $\mathbf{u}_*(t) = \Gamma_{g_*}(t)$ and the best possible system performance for each candidate plant design AEP_*:

$$\begin{aligned} \max_{\mathbf{u}(t)=\Gamma_g(t)} \quad & AEP(v(t), P_w(v)) \\ \text{subject to:} \quad & \mathbf{g_p}(\boldsymbol{\xi}(t), \mathbf{x_{p_*}}) \leq \mathbf{0} \\ & \|\lambda(\Omega_r(t), v(t)) - \lambda_{\text{opt}}(\Omega_r(t), v(t))\| = 0. \\ \text{where:} \quad & \dot{\boldsymbol{\xi}}(t) = \mathbf{f}(\boldsymbol{\xi}(t), \mathbf{x_p}, \mathbf{u}(t)) \end{aligned} \tag{17}$$

Simultaneous formulation Finally, the simultaneous co-design formulation is:

$$\begin{aligned} \max_{[\mathbf{x_p}, \mathbf{u}(t)]} \quad & AEP(v(t), P_w(v)) \\ \text{subject to:} \quad & \mathbf{A_g x_p} \leq \mathbf{0} \\ & \mathbf{g_p}(\boldsymbol{\xi}(t), \mathbf{x_p}) \leq \mathbf{0} \\ & \|\lambda(\Omega_r(t), v(t)) - \lambda_{\text{opt}}(t)(\Omega_r(t), v(t))\| = 0 \\ & \mathbf{0} < \mathbf{x_l} \leq \mathbf{x_p} \leq \mathbf{x_u}. \\ \text{where:} \quad & \dot{\boldsymbol{\xi}}(t) = \mathbf{f}(\boldsymbol{\xi}(t), \mathbf{x_p}, \mathbf{u}(t)) \end{aligned} \tag{18}$$

and $\mathbf{u}(t) = \Gamma_g(t)$.

In this case study two operational modes of FAST (Jonkman and Buhl 2005) are used: 1) Simulation mode: where the forward simulation of system dynamics can be performed to obtain the evolution of state trajectories, and 2) Linearization mode: where the linearized time invariant (but plant dependent) system matrices $\mathbf{A}(\mathbf{x_p})$ and $\mathbf{B}(\mathbf{x_p})$ are extracted from FAST. The matrices $\mathbf{A}(\cdot)$ and $\mathbf{B}(\cdot)$ can be related to system dynamic equations as: $\dot{\boldsymbol{\xi}}(t) = \mathbf{f}(\boldsymbol{\xi}(t), \mathbf{x_p}, \mathbf{u}(t)) \approx \mathbf{A}(\mathbf{x_p}) \cdot \boldsymbol{\xi}(t) + \mathbf{B}(\mathbf{x_p}) \cdot \mathbf{u}(t)$.

The simulation mode is used in structural design portion of the sequential design method (10). The linearization mode, however, is used in conjunction with the inner loop optimal control problem of the nested co-design approach (17) and the simultaneous co-design problem (18). Figure 5 illustrates how FAST's linearization mode is used in conjunction with an optimization algorithm to solve the co-design problem. Design and state variables (as operating points), as well as fixed model parameters $\mathbf{p}$, are passed to FAST from the optimization algorithm. FAST then returns the power production as a function of wind speed and constraint function values. Power production information is then used to compute the objective function value, i.e. AEP.

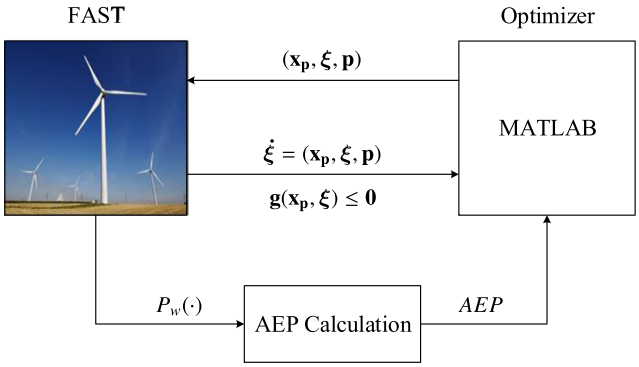

Fig. 5 Information flow in the co-design problem

Once the system dynamic equations are obtained, Problems (17) and (18) are then transcribed to a nonlinear program (NLP) using the Direct Transcription method explained in Section 3. The resulting NLP is then solved using the interior-point algorithm of the `fmincon` solver in MATLAB®.

5 Results and discussion

The AEP maximization problem was solved for each of the three formulations: Sequential Design, Nested Co-Design, and Simultaneous Co-Design. The results are reported in this section. The simulations were performed for a wind speed profile based on a Weibull distribution with parameters: $k = 1.91$, $c = 6.80$, and a mean wind speed of $v_{\text{mean}} = 6.03\ m/s$. Table 3 shows the optimal plant design vector $\mathbf{x_{p_*}}$ for each design formulation. AEP for both co–design formulations is 3231.5 kW·h (demonstrating mathematical equivalence), whereas the sequential design formulation achieved only 2996.9 kW·h. The co-design solution is 8.03% larger than the sequential design result, which is a very significant increase (particularly for higher–capacity turbines). This AEP increase can be attributed to the ability of co-design to capitalize on the strong interdependence between plant and control design with respect

Table 3 Optimal plant design vector and AEP resulting from each design formulation

$\mathbf{x}_{\mathbf{p}_*}$	Sequential	Nested	Simultaneous
D_h (m)	1.81	2.33	2.33
D_r (m)	68.58	69.51	69.51
H_t (m)	76.87	76.66	76.66
$t_w - \text{CP}$ (deg)	[13.72, 5.60, 1.40, −1.70, −5.14]	[12.17, 3.99, −0.53, −3.51, −6.18]	[12.17, 3.99, −0.53, −3.51, −6.18]
$c - \text{CP}$ (m)	[1.38, 1.14, 0.66, 0.55, 0.14]	[1.39, 1.19, 0.73, 0.68, 0.14]	[1.39, 1.19, 0.73, 0.68, 0.14]
$t_h - \text{CP}$ (m)	[0.11, 0.25, 0.48]	[0.16, 0.48, 0.77]	[0.16, 0.48, 0.77]
AEP (kW·h)	2996.9	3231.5	3231.5
% AEP Improvement	–	8.03	8.03
Total Function Evals	331	713	1259

to AEP. The capability of identifying system-optimal solutions, and corresponding performance improvements, motivate greater utilization of integrated co-design methods in development of actively controlled engineering systems. Table 3 lists the number of function evaluations required for sequential design (331), nested co-design (713), and simultaneous co-design (1,259).

Plant design variables dictate turbine size, which has direct impact on energy production capability (cf. (1) and (3)), but structural constraints are more challenging to satisfy for larger turbines. Co-design helps to balance tradeoffs such as this to produce better system performance. Physical system design is tailored to work in concert with control system dynamics, and control systems can be designed in a way that makes satisfaction of physical design requirements easier. For example, the optimal torque trajectory obtained via co-design not only helps maintain an optimal tip speed ratio, but also helps to keep structural deflections and stress more manageable. More specifically, the co-design solution results in an overall deducting in rotor speed, which helps reduce structural deflections. Because control design helped to ease plant constraint satisfaction, there was more flexibility in plant design, supporting the design of a plant that helped to further improve AEP. These synergistic effects are only available when plant and control design coupling are considered explicitly in a design strategy, as is the case with co-design.

Optimal geometric blade design is critically important for AEP improvement as it influences power coefficient characteristics directly. This observation helps to further explain the effectiveness of co-design strategies. In sequential design, AEP can only be improved by adjusting blade geometry during plant design optimization. After plant optimization, the best result that control optimization can achieve is to control rotor speed in a way such that $C_p(t) = C_p(\lambda_{\text{opt}}(t), \beta)$. In other words, the control optimization problem is simply a trajectory matching problem. In contrast, when a co-design approach is used, there is an additional mechanism for increasing AEP. Traversing both design spaces simultaneously allows us to adjust control

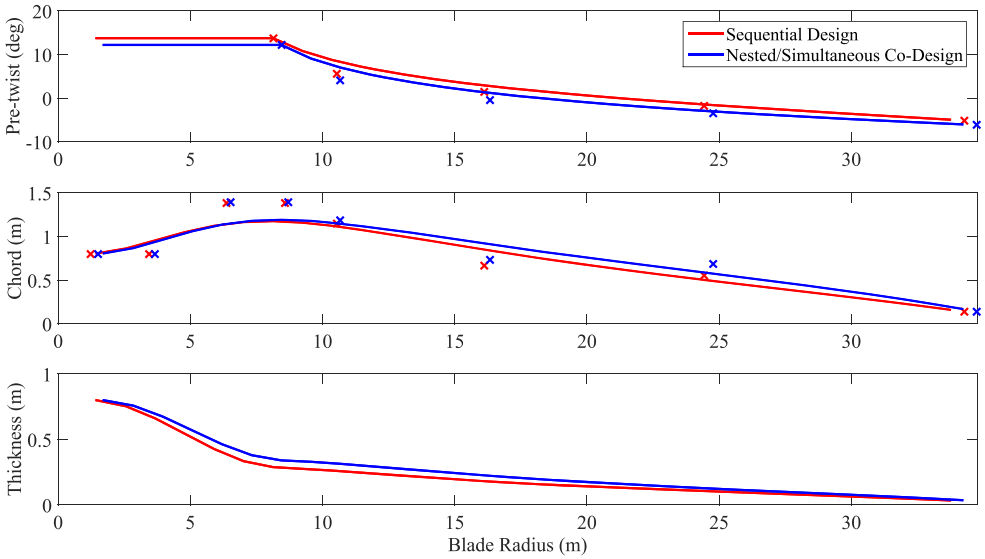

Fig. 6 Optimal blade geometry using control points (shown by ×) for sequential design and nested/simultaneous co-design

design in a way that makes possible the exploration of different plant designs with the potential for higher AEP, as opposed to just funding a control design that enables the turbine to match the optimal power coefficient trajectory. In other words, in co-design, control design decisions are not just useful for matching $C_p(\lambda_{\text{opt}}(t), \beta)$, but also changing $C_p(\lambda_{\text{opt}}(t), \beta)$ in a way that increases AEP by providing more flexibility to plant design. Put another way, sequential design approaches constrain the design space artificially by fixing plant design before control design is considered, whereas co-design supports exploration of a much larger design space through simultaneous plant and control design.

The enhanced flexibility of plant design is observable in this case study. The blade geometry for sequential and co-design approaches are fundamentally different, as shown in Fig. 6 and Table 3. Co-design allows the optimization algorithm to choose larger blade (34.76 m vs. 34.29 m for sequential design) and chord lengths compared to sequential design (cf. Table 3). This results in higher swept area, better aerodynamic performance, and a resulting increase in AEP. Larger blades are made possible in co-design because adjustments to control design make possible the satisfaction of structural constraints (in addition to maintaining an optimal power coefficient).

The co-design solution provides both the optimal plant design and optimal open-loop control (rotor speed) trajectories. This optimal speed trajectory can be used as a guide to design an implementable closed-loop control system that aims to produce approximately the same performance as with optimal open-loop control. Bridging the gap between results generated by co-design with DT and implementable closed-loop control system design is an important topic for future work that will help position co-design methods as practical solutions for integrated design in engineering practice.

6 Conclusion

This article presented a novel approach for optimizing wind turbine design using a co-design method to achieve system optimal solutions. Solution of this problem provides significant insight via exploration of design alternatives that are overlooked when using conventional sequential design. The co-design approaches presented here (nested and simultaneous) involve balanced formulations that treat plant design in a comprehensive manner, including use of nonlinear plant design constraints and bi-directional coupling. Balanced co-design is essential for producing more meaningful solutions to multidisciplinary optimization problems for dynamic systems. The co-design approaches produced system-optimal designs that resulted in a performance improvement of more than eight percent compared to sequential design optimization. More importantly, the specific mechanisms that made these design improvements possible for the wind turbine design case study were identified and discussed. Applying co-design to wind turbine design optimization enables the use of control design to support the satisfaction of challenging structural constraints. This in turn gives rise to greater design freedom in the plant design space, leading to larger blade designs that increase maximum AEP while satisfying structural constraints.

Acknowledgments This work was partially supported by the Clean Energy Education and Research Fellowship awarded to first author by the Graduate College at the University of Illinois at Urbana-Champaign. This support is gratefully acknowledged.

References

Allison JT (2013) Plant-limited co-design of an energy-efficient counterbalanced robotic manipulator. ASME J Mech Des 135(10):101,003

Allison JT, Herber DR (2014) Multidisciplinary design optimization of dynamic engineering systems. AIAA J 52(4):691–710

Allison JT, Guo T, Han Z (2014) Co-design of an active suspension using simultaneous dynamic optimization. ASME J Mech Des 136(8):081,003

Ashuri T, Zaaijer MB, Martins JRRA, van Bussel GJW, van Kuik GA (2014) Multidisciplinary design optimization of offshore wind turbines for minimum levelized cost of energy. Renew Energy 68:893–905

Bajodah AH (2005) Nonminimal kane's equations of motion for multibody dynamical systems subject to nonlinear nonholonomic constraints. Multibody System Dynamics 14(2):155–187

Benini E, Toffolo A (2002) Optimal design of horizontal-axis wind turbines using blade-element theory and evolutionary computation. Journal of Solar Energy Engineering 124(4):357–363

Betts JT (2010) Practical methods for optimal control and estimation using nonlinear programming. SIAM, Philadelphia

Biegler LT (2010) Nonlinear programming: concepts, algorithms, and applications to chemical processes. SIAM

Boukhezzar B, Lupu L, Siguerdidjane H, Hand M (2007) Multivariable control strategy for variable speed, variable pitch wind turbines. Renew Energy 32:1273–1287

Bryson AE, Ho YC (1975) Applied optimal control: optimization, estimation and control. Taylor & Francis

Burnham A (2009) Variable rotor-resistance control of wind turbine generators. In: Power & energy society general meeting. IEEE, pp 1–6

Chen L, MacDonald E (2012) Considering landowner participation in wind farm layout optimization. J Mech Des 134:084,506

Chen L, MacDonald E (2014) A system-level cost-of-energy wind farm layout optimization with landowner modeling. Energy Convers Manag 77:484–494

Chowdhury S, Messac A, Zhang J, Castillo L, Lebron J (2010) Optimizing the unrestricted placement of turbines of differing rotor diameters in a wind farm for maximum power generation. In: ASME 2010 international design engineering technical

conferences and computers and information in engineering conference, Montreal
Chowdhury S, Zhang J, Messac A, Castillo L (2012) Unrestricted wind farm layout optimization (uwflo): investigating key factors influencing the maximum power generation. Renew Energy 38:16–30
Chowdhury S, Tong W, Messac A, Zhang J (2013a) A mixed-discrete particle swarm optimization algorithm with explicit diversity-preservation. Struct Multidiscip Optim 47(3):367–388
Chowdhury S, Zhang J, Messac A, Castillo L (2013b) Optimizing the arrangement and the selection of turbines for wind farms subject to varying wind conditions. Renew Energy 52:273–282
Cramer EJ, Dennis JE, Frank PD, Lewis RM, Shubin GR (1993) Problem formulation for multidisciplinary optimization. SIAM J Optim 4:754–776
Dang DQ, Wu S, Yang W, Cai W (2009) Model predictive control for maximum power capture of variable speed wind turbines. In: IEEE international conference on control and automation, Christchurch
Dang DQ, Wu S, Yang W, Cai W (2010) Ieee international conference on control and automation. In: IPEC2010
DOE (2008) 20 % wind energy by 2030: Increasing wind energy's contribution to u.s. electricy supply. Tech. Rep. DOE/GO-102008-2567, US Department of Energy, http://www.nrel.gov/docs/fy08osti/41869.pdf
DuPont BL, Cagan J (2012) An extended pattern search approach to wind farm layout optimization. J Mech Des 134(8):081,002
Fathy H, Reyer J, Papalambros P, Ulsoy AG (2001) On the coupling between the plant and controller optimization problems. In: 2001 American control conference. IEEE, pp 1864–1869
Forcier LC, Joncas S (2012) Development of a structural optimization strategy for the design of next generation large thermoplastic wind turbine blades. Struct Multidiscip Optim 45(6):889–906
Giguere P, Selig MS, Tangler JL (1999) Blade design trade-offs using low-lift airfoils for stall-regulated hawts. Journal of Solar Energy Engineering:217–223
He Y, Monahan AH, Jones CG, Dai A, Biner S, Caya D, Winger K (2010) Probability distributions of land surface wind speeds over north america. J Geophys Res Atmos 115(D4):1–9
Holley WE (2003) Wind turbine dynamics and control: Issues and challenges. In: American control conference, Denver
Jonkman J (2009) Dynamics of offshore floating wind turbines - model development and verification. Wind Energy:459–492
Jonkman J, Buhl M (2004) New developments for the nwtc's fast aeroelastic hawt simulator. In: 42nd aerospace sciences meeting and exhibit conference. AIAA, Reno
Jonkman JM, Buhl ML (2005) Fast user's guide. Tech. Rep. NREL/EL-500-38230, National renewable energy laboratory
Jureczko M, Pawlak M, Mezyk A (2005) Optimisation of wind turbine blades. J Mater Process Technol:463–471
Kusiak A, Li W, Song Z (2010) Dynamic control of wind turbines. Renew Energy:456–463
Lu S, Kim HM (2014) Wind farm layout design optimization through multi-scenario decomposition with complementarity constraints. Eng Optim 46(12):1669–1693
Maalawi KY, Negm HM (2002) Optimal frequency design of wind turbine blades. J Wind Eng Ind Aerodyn:961–986
Martins JRRA, Lambe AB (2013) Multidisciplinary design optimization: a survey of architectures. AIAA J 51:2049–2075
Moriarty P, Hansen A (2005) Aerodyn theory manual. Technical Report NREL/TP-500-36881, National Renewable Energy Laboratory
Muljadi E, Butterfield CP (2001) Pitch-controlled variable-speed wind turbine generation. IEEE Trans Ind Appl 37(1):240–246
Munteanu I, Bratcu AI, Cutululis NA, Ceanga E (2008) Optimal control of wind energy systems. Advances in industrial control. Springer, London, pp 76–77
Namik H, Stol K (2011) Performance analysis of individual blade pitch control of offshore wind turbines on two floating platforms. Mechatronics 21(4):691–703
Negm HM, Maalawi KY (2000) Structural design optimization of wind turbine towers. Comput Struct:649–666
Nicholson JC (2011) Design of wind turbine tower and foundation systems: optimization approach. Master's thesis. University of Iowa, USA
Pontryagin LS (1962) The mathematical theory of optimal processes. Interscience
Quarton DC (1998) The evolution of wind turbine design analysis-a twenty year progress review. Wind Energy 1:5–24
Reyer J, Fathy H, Papalambros P, Ulsoy A (2001) Comparison of combined embodiment design and control optimization strategies using optimality conditions. In: Conferences InternationalDesignEngineeringTechnical, Renaud JE (eds) ASME, pp 1023–1032
Sale D (2010) Harp-opt user's guide. Nwtc design codes, National Renewable Energy Laboratory, http://wind.nrel.gov/designcodes/simulators/HARP_Opt
Scholbrock A, Fleming P, Fingersh L, Wright A, Schlipf D, Haizmann F, Belen F (2013) Field testing lidar-based feed-forward controls on the nrel controls advanced research turbine. In: 51st AIAA Aerospace Sciences Meeting including the New Horizons Forum and Aerospace Exposition, American Institute of Aeronautics and Astronautics
Sobieszczanski-Sobieski J, Haftka RT (1997) Multidisciplinary aerospace design optimization: survey of recent developments. Structural optimization 14(1):1–23
Soltani M, Wsniewski R, Brath P, Boyd S (2011) Load reduction of wind turbines using receding horizon control. In: International Conference on Control Applications (CCA), Denver
Stotsky A, Egardt B (2013) Individual pitch control of wind turbines: Model-based approach. Proc IMechE Part I J Syst Control Eng 227(7):602–609
Thiringer T, Linders J (1993) Control by variable rotor speed of a fixed-pitch wind turbine operating in a wide speed range. Transactions on Energy Conversion 8(3):520–526
Uys P, Farkas J, Jármai K, van Tonder F (2007) Optimisation of a steel tower for a wind turbine structure. Eng Struct 29(7):1337–1342
Wan Z, Kothare MV (2003) An efficient off-line formulation of robust model predictive control using linear matrix inequalities. Automatica 39(5):837–846
Wang Y, Boyd S (2010) Fast model predictive control using online optimization. IEEE Trans Control Syst Technol 18(2):267–278
Xudong W, Shen WZ, Zhu WJ, Sorensen JN (2009) Shape optimization of wind turbine blades. Wind Energy:781–803
Yoshida S (2006) Wind turbine tower optimization method using a genetic algorithm. Wind Eng 30(6):453–469
Zakhama R, Abdalla MM (2010) Wind load modeling for topology optimization of continuum structures. Struct Multidiscip Optim 42(1):157–164
Zeid I (1991) CAD/CAM theory and practice. McGraw-Hill series in mechanical engineering, McGraw-Hill